

# Analysis of Gas-Phase Clusters Made from Laser-Vaporized Icosahedral Al–Pd–Mn

J. A. Barrow, D. J. Sordelet, M. F. Besser, C. J. Jenks, and P. A. Thiel\*

Ames Laboratory and Department of Chemistry, Iowa State University, Ames, Iowa 50011

E. F. Rexer and S. J. Riley

Chemistry Division, Argonne National Laboratory, Argonne, Illinois 60439

Received: February 19, 2002; In Final Form: May 6, 2002

An icosahedral Al–Pd–Mn quasicrystal sample is laser vaporized to form metal clusters by gas aggregation. The clusters are subsequently laser ionized and mass analyzed in a time-of-flight mass spectrometer. The mass spectra show cluster compositions which are qualitatively similar to that of the sample. This is consistent with a kinetically controlled cluster growth process. Cluster thermodynamic stability is probed by multiphoton ionization/fragmentation, which induces primarily Al and Mn loss. The resulting spectra are composed of a series of Pd-rich Al–Pd clusters. The average cluster composition is 60 ( $\pm 1$ )% Pd. This composition is close to a known eutectic in the Al–Pd system. When manganese is seen on these clusters, it is always in units of  $\text{Mn}_3$ . These results are discussed in terms of relative binding strengths in the Al–Pd–Mn alloy system.

## Introduction

In 1982, Shechtman et al. characterized an aluminum-rich intermetallic compound with a rotational symmetry forbidden by classical crystallography.<sup>1</sup> Since then, it has been shown that such forbidden symmetries are the result of well-ordered but aperiodic atomic structures. This new form of matter is neither crystalline nor amorphous, but is quasiperiodic and has been termed quasicrystalline. In comparison with crystalline intermetallics, quasicrystals exhibit peculiar physical and electronic properties.<sup>2</sup> For example, quasicrystals are very hard and brittle, and they have low surface energy and low electrical and thermal conductivities. The relationship between quasiperiodicity and these unique properties has not been firmly established, but there have been extensive research efforts aimed at understanding this relationship.

Theoretical models have been proposed using either pseudo-Mackay icosahedral or Bergman type clusters as a basic motif for the quasicrystalline structure.<sup>3–5</sup> The Bergman type cluster model requires one cluster with the composition  $\text{Al}_{23}\text{Pd}_7\text{Mn}_3$ .<sup>5</sup> The pseudo-Mackay cluster model uses three different types of basic clusters:  $\text{Al}_{38}\text{Pd}_7\text{Mn}_6$ ,  $\text{Al}_{31}\text{Pd}_{20}$ , and  $\text{Al}_{30}\text{Pd}_{21}$ .<sup>3,4</sup> There is experimental evidence to support the idea of cluster-based structures. Measurements of the electrical and thermal properties of quasicrystals suggest a hierarchical localization. This is consistent with the electron localization inherent to a cluster.<sup>4</sup> In addition, the cleavage properties and plasticity of quasicrystals have been interpreted in the context of stable clusters acting as structural subunits.<sup>6,7</sup>

It is possible to describe the bulk structure of quasicrystalline materials with cluster models, but the models require complex rules for overlapping and interlacing the clusters,<sup>4</sup> and it is difficult to explain how clusters would actually assemble during growth to form a quasicrystalline structure. With this in mind, we felt that a study of isolated clusters of quasicrystalline material might probe the fundamental interactions between the

atomic species in quasicrystals and improve our understanding of their local electronic properties and geometric structure. As a basis for such a study, we have applied a proven technique for investigating the properties of gas-phase metal clusters—laser vaporization coupled with time-of-flight mass spectrometry (TOF-MS).<sup>8,9</sup> In the present study an icosahedral  $\text{Al}_{70}\text{Pd}_{22}\text{Mn}_8$  quasicrystalline target is laser vaporized in a conventional cluster source and the composition and stability of the resulting clusters are probed via laser ionization TOF-MS. Although studies of pulsed-laser deposition of quasicrystalline materials have been reported,<sup>10</sup> there have not been to our knowledge any cluster beam studies of the Al–Pd–Mn quasicrystal system or of any of the possible two-component systems Al–Pd, Al–Mn, or Mn–Pd.

## Experimental Section

The experimental apparatus has been described in detail elsewhere.<sup>11,12</sup> To summarize briefly, gas-phase clusters are produced by laser vaporization in a source coupled to a flow tube reactor (FTR). The Al–Pd–Mn target rod is vaporized using a frequency-doubled Nd:YAG laser. Helium gas continuously flows through the source and carries the vaporization plume through the FTR. This results in rapid cooling of the plume and the condensation of atoms into clusters. The clusters then pass out of a nozzle at the end of the FTR and through a conical skimmer to form a molecular beam. The beam then enters a separate chamber where the clusters are laser ionized and the ions extracted into the time-of-flight mass spectrometer. The mass spectrometer can be operated in two modes: direct (linear) and reflectron. In the linear mode, an ion's flight time is determined solely by its velocity, i.e., its initial mass and the extraction energy. Any metastable cluster post-source decay (PSD, the breakup of cluster ions in the drift region) will not be evident in the mass spectrum, since the daughter ions will have the same velocity as their parents. In the reflectron mode (which provides superior resolution), ion flight time also depends on translational energy, so daughter ions resulting from metastable PSD, having energies different from their parents, will

\* Corresponding author. E-mail: thiel@ameslab.gov.

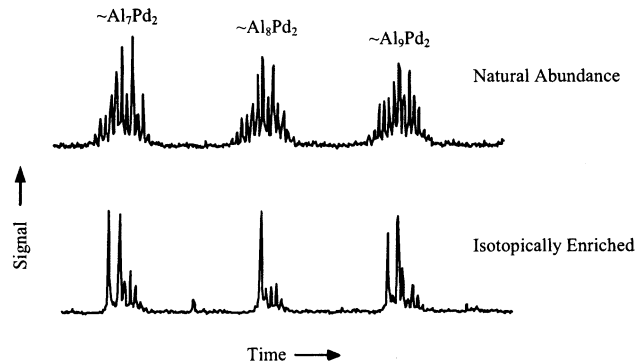


**Figure 1.** Portions of time-of-flight mass spectra recorded for a natural Al–Pd–Mn target (upper), and an isotopically enriched Al– $^{106}\text{Pd}$ –Mn target (lower).

appear as additional peaks in the mass spectrum. Metastable cluster decay can thus be identified by comparing linear TOF-MS data to reflectron TOF-MS data.

Clusters are ionized with an excimer laser under conditions of either single-photon or multiphoton absorption. For single-photon ionization (SPI) experiments, a low fluence ( $1.3 \times 10^{16}$  photons/cm $^2$ ) ArF excimer laser (193 nm, 6.42 eV photon energy) is used. Under these conditions, it is assumed that the distribution of cluster ion species directly reflects the distribution of neutral clusters that exit the source. The validity of this assumption has been tested over many years of cluster research, and has been shown to be good, provided the photon energy is not substantially larger than the cluster ionization potential (IP). In general, SPI mass spectra have very good resolution, and they are used to make mass peak assignments. But even with very high resolution, definitive mass assignments rapidly become impossible with increasing cluster size because of the five significant Pd isotopes (Al and Mn have only one isotope each). To help solve this problem, a target is made from isotopically enriched  $^{106}\text{Pd}$ , by sintering quasicrystalline Al– $^{106}\text{Pd}$ –Mn powder. A detailed description of the sample fabrication procedure has been reported.<sup>11</sup> Figure 1 shows mass spectra illustrating the simplification provided by the isotopic enrichment.

Even with the  $^{106}\text{Pd}$ -enriched target, isobaric interferences occur. For example,  $^{27}\text{Al}_8^{106}\text{Pd}$  and  $^{106}\text{Pd}_2^{55}\text{Mn}_2$  have the same nominal mass. Modeling the SPI spectra helps compensate for these interferences. First, “best guess” peak assignments are made for the spectrum obtained with the isotopically enriched target. Using these assignments and the known isotopic distribution of natural Pd, a natural abundance mass spectrum is simulated. The simulated spectrum is then compared with an experimental natural abundance mass spectrum. This process is iterated until the two spectra agree. The peak assignments that produce the best fit are taken as the correct ones.

In multiphoton ionization (MPI) experiments the clusters are ionized with a high-fluence ( $1.3 \times 10^{17}$  photons/cm $^2$ ) excimer laser whose single-photon energy can be below the cluster IPs. In the present experiments both the ArF and a XeCl (308 nm, 4.03 eV photon energy) laser were used for MPI. The multiphoton absorption leads to extensive cluster fragmentation, so that the prominent peaks in an MPI spectrum are due to particularly stable fragment (daughter) species. This provides a means of identifying thermodynamically stable cluster species. This is essential for a detailed analysis of the binding patterns in the Al–Pd–Mn system. Some peak broadening is seen in MPI mass spectra due to the random velocity vectors imparted to the daughters during the fragmentation process.

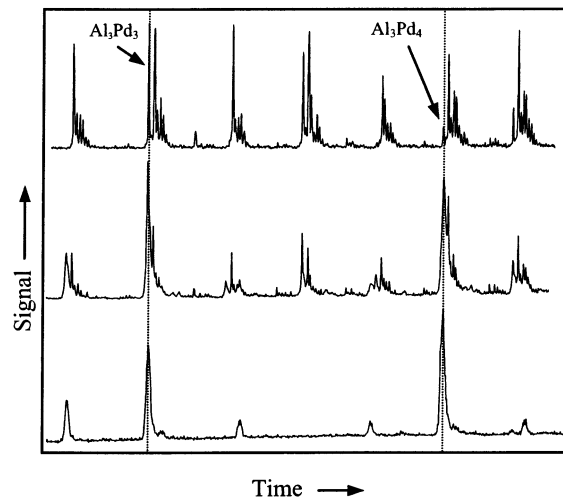


**Figure 2.** Top panel: portion of the mass spectrum recorded with low ionizing laser fluence ( $1.3 \times 10^{16}$  photons/cm $^2$ ) and the isotopically enriched target. Middle panel: same spectrum recorded with intermediate laser fluence ( $3.3 \times 10^{16}$  photons/cm $^2$ ). Lower panel: the spectrum recorded with high laser fluence ( $1.3 \times 10^{17}$  photons/cm $^2$ ).

## Results and Interpretation

The SPI spectrum shows a broad, uniform distribution of mass peaks periodically grouped into envelopes separated by  $\sim 27$  amu. This is representative of the similar mass multiples of Al, Mn, and Pd. A small portion of this distribution is shown in the top spectrum of Figure 2. There is no observable modulation of the envelope intensity in the vicinity of the masses of Bergman or pseudo-Mackay icosahedral clusters that would indicate any special stability of these species. This is not surprising, since clusters that are made in a laser vaporization/inert gas condensation source grow via a process that is strongly kinetically controlled. The amount of a given cluster produced does not depend on that cluster’s stability, but only on the statistical probability that sufficient (irreversible) cluster-atom collisions occur to make that cluster.<sup>13</sup> Traditional “magic numbers” do not appear in mass spectra of clusters made in this manner. Instead, other probes of cluster thermodynamic stability must be used.<sup>13–16</sup> We applied three of these probes:<sup>17</sup> heating the clusters to 1000 °C, to look for thermal fragmentation, photoionizing them nearer to their ionization thresholds to identify clusters with unusually high IPs, and reacting them with oxygen, another probe of electronic stability. In no case was there any evidence for special behavior in the vicinity of the Bergman or pseudo-Mackay icosahedral clusters. In fact, the initial broad, uniform distribution of mass peak intensities was generally unchanged when these probes were applied.

The situation is dramatically different when the clusters are multiphoton ionized. A very strong modulation of the overall intensity distribution occurs, as can be seen in the bottom spectrum of Figure 2. As discussed above, this modulation is due to extensive cluster fragmentation, and the prominent peaks represent stable daughter species. This signal modulation pattern extends to the largest clusters studied, but once again there is no obvious change in the pattern in the vicinity of Bergman and pseudo-Mackay clusters. It should be noted that even though the spectral peaks are too broad to be resolved, it is still possible to observe an increase in signal intensity near the mass of a particular species.

As mentioned above, MPI causes peak broadening in the spectra, complicating mass assignments. This is resolved by recording the spectrum at an intermediate fluence, as is shown in the middle spectrum of Figure 2. Here the stable daughter

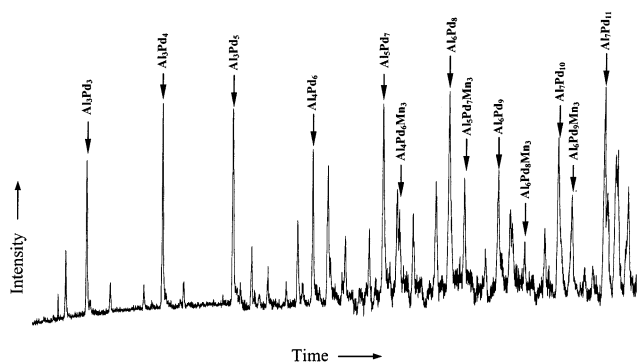


**Figure 3.** Representative portion of the MPI mass spectrum from the isotopically enriched target. Ionization is with a focused XeCl laser. Principal peaks showing the progression of  $\text{Al}_m\text{Pd}_n$  species, as well as some of the  $\text{Mn}_3$ -containing peaks, are annotated.

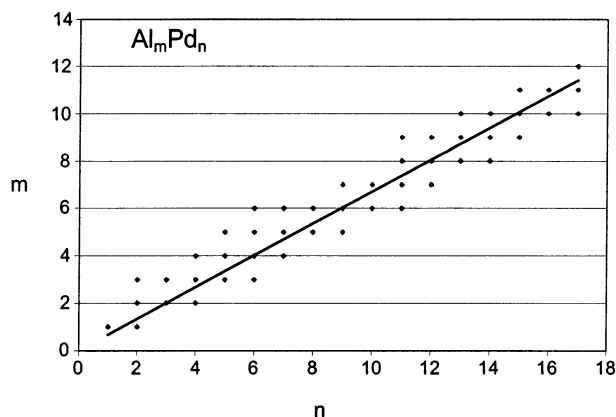


**Figure 4.** Plot of the number of Al atoms,  $m$ , vs the number of Pd atoms,  $n$ , in MPI-produced clusters. The straight line is a linear regression with a slope of 0.67 ( $R^2 = 0.91$ ) corresponding to an average cluster composition of 60% Pd.

peaks have begun to grow in intensity and have broadened somewhat, but not so much that unambiguous comparison with the top spectrum cannot be made. Also, since the laser fluence is not yet high enough to multiphoton ionize all of the clusters, SPI clusters are still present in the spectrum. By aligning the three spectra, it is possible to determine which SPI peaks are coincident with the MPI peaks. It is assumed that coincident peaks represent clusters of the same composition. In this manner, conclusive composition assignments can be made for peaks in the lower mass region of the MPI spectrum. This region, along with some of the assignments, is shown in Figure 3.

This analysis shows that the principle peaks in the MPI spectrum are due to Pd-rich,  $\text{Al}_m\text{Pd}_n$  clusters. For most values of  $n$ , there is a distribution of three  $m$  values. This is shown in Figure 4, where the data are plotted as  $m$  vs  $n$ , i.e., number of Al atoms in the cluster vs number of Pd atoms in the cluster. Each data point represents a specific  $\text{Al}_m\text{Pd}_n$  cluster. Average cluster composition is determined by linear regression, yielding a slope of 0.67 with an  $R^2$  value of 0.91. This corresponds to an average Pd concentration of 60 ( $\pm 1$ )%. This composition is coincident with a known Al–Pd eutectic at 61.3%.<sup>18</sup>

Manganese begins to appear consistently on clusters sizes of  $\text{Al}_m\text{Pd}_6$  and greater, but only as  $\text{Mn}_3$ . Manganese addition is not observed with either more or less than three Mn atoms. This suggests that the stable  $\text{Al}_m\text{Pd}_n$  clusters may be decorated with a Mn trimer.

It is difficult to determine relative  $\text{Al}_m\text{Pd}_n\text{Mn}_3$  and  $\text{Al}_m\text{Pd}_n$  peak intensities due to MPI broadening and mass overlap. By fitting the measured peaks with Lorentzian profiles, it is possible

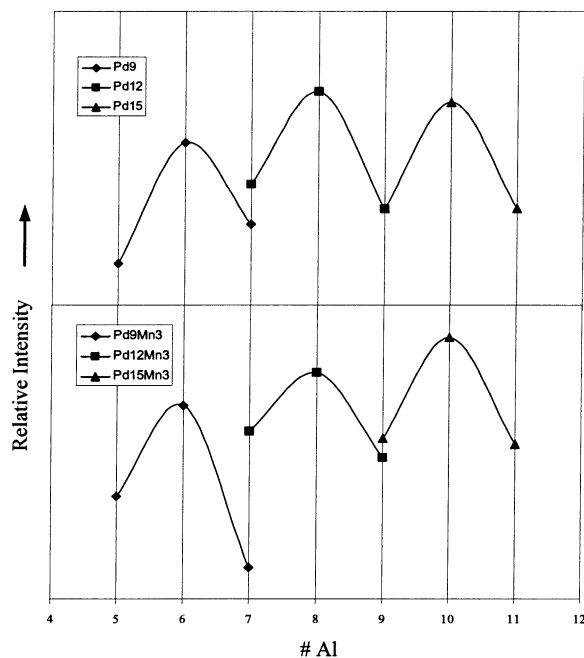


**Figure 5.** Intensity distributions of representative  $\text{Al}_m\text{Pd}_n$  species derived from peaks without (upper panel) and with (lower panel)  $\text{Mn}_3$  attached.

to deconvolute them and recover the relative peak intensity distributions. These are shown in Figure 5. Each vertical pair of curves represents a single value of  $n$ , i.e., they represent clusters with the same number of Pd atoms. Each curve spans a series of  $m$  values, i.e., it spans clusters over a range of number of Al atoms. The top and bottom curves compare clusters with and without Mn, respectively. Comparing each vertical pair of curves, it can be seen that the intensity profiles derived from  $\text{Al}_m\text{Pd}_n$  peaks match those derived from  $\text{Al}_m\text{Pd}_n\text{Mn}_3$  peaks. This indicates that the  $\text{Mn}_3$  acts as a chemical spectator that can attach or detach from the  $\text{Al}_m\text{Pd}_n$  cluster without perturbing the Al–Pd stoichiometry.

This spectator role for manganese is reinforced by a comparison of MPI spectra of clusters made from the Al–Pd–Mn target with those of Al–Pd clusters made in a general purpose alloy cluster source.<sup>19</sup> In the latter source, two YAG laser beams are used to vaporize metal from a target rod and a wire suspended near the rod. By adjusting the relative power and timing of the laser pulses, the relative amounts of the two metals in the vaporized plume can be varied. Figure 6 shows, in the upper panel, a portion of the MPI spectrum recorded with an Al rod and a Pd wire as the source. Further, these data are obtained under conditions that produce SPI spectra qualitatively similar to those from the quasicrystal target (i.e., the alloy clusters are Al-rich and have comparable relative amounts of Al and Pd in them). The lower panel in Figure 6 shows an MPI spectrum recorded under similar conditions for the quasicrystal target. The virtually identical appearance of the two spectra supports the argument that the presence of Mn in the initial cluster has little if any effect on the compositions of the ultimately stable  $\text{Al}_m\text{Pd}_n$  species.

A comparison of reflectron TOF MPI spectra with linear TOF MPI spectra shows no evidence for metastable decay of clusters from the quasicrystalline target rod. This is somewhat surprising, since the primary process occurring in the Al–Pd clusters under MPI conditions is Al loss, while multiphoton ionization of pure aluminum clusters also results in Al loss and shows substantial metastable PSD.<sup>20</sup> The difference is in the range of fragment-cluster binding energies in the two systems. In order for

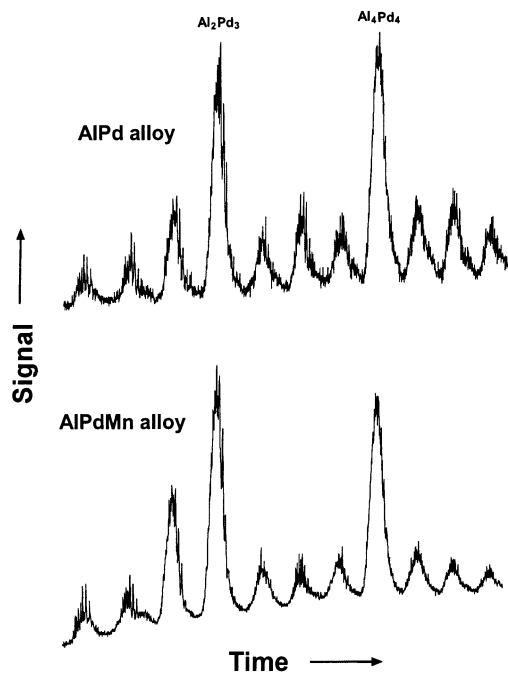


**Figure 6.** Upper panel: portion of the MPI spectrum recorded with an alloy cluster source using a (natural) Pd wire and an Al target rod. Lower panel: same spectrum recorded with the (natural) quasicrystal target. Ionization in both cases is with a focused ArF laser. The slight differences in relative peak intensities reflects a slightly higher laser fluence for the lower spectrum.

metastable PSD to occur, there must be an evaporative event that occurs during the ion flight time in the reflectron. In pure Al clusters, binding energies are relatively independent of cluster size, and the time to decay will depend largely on the amount of excess energy in the activated cluster. Each time a decay event occurs, this energy is reduced by at least the amount of the binding energy, so there will be a nearly continuous distribution of excess energies and thus decay times. One of these times will fall within the window leading to metastable PSD. For the Al–Pd clusters, on the other hand, there is a sudden increase in cluster–Al binding energy when the cluster reaches the stable  $\text{Al}_m\text{Pd}_n$  composition. Apparently, the aluminum (as well as the manganese) loss from the initial clusters is so rapid that these processes are finished before the ions are extracted. Subsequent Al loss, if any, does not occur within the flight time, so no metastable PSD peaks appear in the MPI mass spectra.

## Discussion

The two types of laser ionization conditions used here, SPI and MPI, provide information about two processes: formation and decay of the clusters. It is reasonable, and consistent with previous work, to expect that the cluster formation is dominated by the kinetics of the cluster–atom collisions, whereas decay (as probed with MPI) provides information about the relative thermodynamic stabilities of the decay products.<sup>21</sup>

The kinetic formation of Al-rich clusters in the FTR is consistent with the Al-rich plume composition expected when vaporizing the quasicrystalline target. Beyond this, the SPI data do not provide fundamental insight into the cluster chemistry. They are, however, essential in identifying the MPI spectral peaks correctly, as illustrated in Figure 2.

During the multiphoton ionization process the clusters quickly lose the Mn and then begin to lose Al until a stable Pd core is

formed. This idea is consistent with the relative vapor pressures of the three metals:  $\text{Mn} > \text{Al} > \text{Pd}$ .

The average composition of the Al–Pd clusters is  $60 (\pm 1)\%$  Pd. This may be related to the existence of a eutectic in the Al–Pd phase diagram at 61.3% Pd.<sup>18</sup> Although these are gas-phase clusters, it is not unreasonable to think of them as liquid droplets from which the aluminum species “boil off”, allowing the cluster to approach the eutectic by following the bulk liquidus. While this idea is intriguing, it clearly requires further research before conclusions may be drawn.

It is unclear whether the Al plays a role in stabilizing the core, or simply decorates a stable Pd core. The similarity of the intensity profiles for  $\text{Al}_m\text{Pd}_n$  clusters and  $\text{Al}_m\text{Pd}_n\text{Mn}_3$  clusters (Figure 5) suggests that Mn addition occurs after the  $\text{Al}_m\text{Pd}_n$  has formed. Since the  $\text{Mn}_3$  does not affect the Al–Pd stoichiometry, it is probable that Mn acts only as a chemical spectator and has no role in core stabilization.

The fact that Mn is observed only in groups of 3 per cluster is interesting. It suggests that the Mn atoms may be linked together to form a trimer. Mn decoration does not occur regularly until the core has reached the critical size of  $\text{Al}_m\text{Pd}_6$ . It may be that  $\text{Mn}_3$  requires a specific binding site on the Al–Pd cluster. This site may not be consistently available until the core has reached the critical size. It is puzzling that we do not observe any Al–Pd clusters with multiples of three Mn. We would expect to find clusters with  $\text{Mn}_6$  or  $\text{Mn}_9$  decoration, but this is not observed.

Returning to the initial motivation for this study, the clusters observed in these experiments are different from those clusters expected from the cluster-based structure of the parent quasicrystal, in two ways. First, a more intense signal corresponding to the Bergman and MacKay-type clusters is not observed under these experimental conditions; hence, there is no evidence that they have special stability, at least not as isolated units. Second, the Mn atoms do not affect the stability of the Al–Pd clusters under MPI conditions, whereas in the bulk quasicrystalline material Mn atoms are integral components. It is possible that for different types of gas-phase cluster experiments, perhaps those more conducive to equilibration of large, multicomponent structures, Bergman or MacKay-type clusters could be observed; however, the present data fail to indicate a special stability for isolated clusters of the type that exist in quasicrystals. It is also possible that such clusters only have special stability in the context of the bulk matrix, and may not exist as isolated units.

**Acknowledgment.** This work is supported by the U.S. Department of Energy, Office of Basic Energy Sciences, Division of Materials Sciences under Contract No. W-405-Eng-82 (Ames Laboratory) and the Division of Chemical Sciences under Contract No. W-31-109-Eng-38 (Argonne National Laboratory).

## References and Notes

- (1) Shechtman, D.; Blech, I.; Gratias, D.; Cahn, J. W. *Phys. Rev. Lett.* **1984**, *53*, 1951–1953.
- (2) Jenks, C. J.; Thiel, P. A. *Langmuir* **1998**, *14*, 1392–1397.
- (3) Janot, C.; de Boissieu, M. *Phys. Rev. Lett.* **1994**, *72*, 1674–1677.
- (4) Janot, C. *Phys. Rev. B: Condens. Matter* **1996**, *53*, 181–191.
- (5) Elser, V. *Philos. Mag. B* **1996**, *73*, 641–656.
- (6) Ebert, P.; Feuerbacher, M.; Tamura, N.; Wollgarten, M.; Urban, K. *Phys. Rev. Lett.* **1996**, *77*, 3827–3830.
- (7) Feuerbacher, M.; Metzmacher, C.; Wollgarten, M.; Urban, K.; Baufeld, B.; Bartsch, M.; Messerschmidt, U. *Mater. Sci. Eng. A* **1997**, *233*, 103–110.
- (8) De Heer, W. A.; Knight, W. D.; Chou, M. Y.; Cohen, M. L. *Solid State Phys.* **1987**, *40*, 93–181.



- (9) Klots, T. D.; Winter, B. J.; Parks, E. K.; Riley, S. J. *J. Chem. Phys.* **1991**, *94*, 8919–8930.
- (10) Teghil, R.; D'Alessio, L.; Simone, M. A.; Zaccagnino, M.; Ferro, D.; Sordelet, D. *J. Appl. Surf. Sci.* **2000**, *168* (1–4), 267–269.
- (11) Barrow, J. A.; Rexer, E. F.; Sordelet, D. J.; Besser, M. F.; Jenks, C. J.; Riley, S. J.; Thiel, P. A. *Proceedings of the Materials Research Society (Symposium K)*; Belin-Ferré, E., Thiel, P. A., Tsai, A.-P., Urban, K., Eds.; Material Research Society, 2000; pp K5.4.1–K5.4.5.
- (12) Parks, E. K.; Riley, S. J. In *The Chemical Physics of Atomic and Molecular Clusters*; Scoles, G., Ed.; North-Holland: Amsterdam, 1990; p 761.
- (13) Riley, S. J. *J. Non-Cryst. Solids* **1996**, *205–207*, 781–787.
- (14) Parks, E. K.; Weiller, B. H.; Bechthold, P. S.; Hoffman, W. F.; Nieman, G. C.; Pobo, L. G.; Riley, S. J. *J. Chem. Phys.* **1988**, *88*, 1622–1632.
- (15) Zhu, L.; Ho, J.; Parks, E. K.; Riley, S. J. *J. Chem. Phys.* **1993**, *98*, 2798–2804.
- (16) Winter, B. J.; Parks, E. K.; Riley, S. J. *J. Chem. Phys.* **1991**, *94*, 8618–8621.
- (17) Riley, S. J.; Kerns, K. P.; Jenks, C. J.; Sordelet, D. J.; Thiel, P. A. The Search for Magic Number Clusters in Laser-Vaporized Al–Pd–Mn. *Book of Abstracts, 7th International Conference on Quasicrystals, Stuttgart, Germany, September 20–24, 1999*.
- (18) *Bulletin of Alloy Phase Diagrams*; American Society for Metals: Metals Park, Ohio, 7 (4), Aug. 1986.
- (19) Rexer, E. F.; Jellinek, J.; Krissinel, E. B.; Parks, E. K.; Riley, S. J. *J. Chem. Phys.* **2002**, *117*, 82–94.
- (20) Rexer, E. F.; Parks, E. K.; Riley, S. J. Unpublished results.
- (21) Martin, T. P.; Bjornholm, S.; Borggren, J.; Bréchnignac, C.; Cahuzac, Ph.; Hansen, K.; Pederson, J. *Chem. Phys. Lett.* **1991**, *186*, 53–57.